Effect of Lewis/Brønsted acid sites in HZSM−5 zeolite on the selectivity of *para*-xylene during methylation of toluene with methanol

Min Han [a], Zhongzhong Xue [a], Lixia Ling [a,b,*], Riguang Zhang [c,d], Maohong Fan [b], Baojun Wang [c,d,*]

[a] *College of Chemistry and Chemical Engineering, Taiyuan University of Technology, Taiyuan030024, Shanxi, China*
[b] *Department of Chemical and Petroleum Engineering, University of Wyoming, 1000 E University Ave, Laramie WY 82071, United States*
[c] *State Key Laboratory of Clean and Efficient Coal Utilization, Taiyuan University of Technology, Taiyuan030024, Shanxi, China*
[d] *Key Laboratory of Coal Science and Technology (Taiyuan University of Technology), Ministry of Education and Shanxi Province, Taiyuan030024, Shanxi, China*

ARTICLE INFO

ABSTRACT

The methylation reaction of methanol and toluene to xylenes has been carried out in Brønsted Acid Sites (BAS)−HZSM−5, AlOH^{2+}/BAS−HZSM−5 and ZnOH$^+$/BAS−HZSM−5 catalysts. The stronger acid strengths are produced in AlOH^{2+}/BAS−HZSM−5 and ZnOH$^+$/BAS−HZSM−5 due to the synergistic effect of Lewis Acid Sites (LAS) and BAS compared to BAS−HZSM−5, which is beneficial to the dissociation of methanol. AlOH^{2+}/BAS−HZSM−5 shows the highest activity for methanol dissociation with the strongest acid strength. The Gibbs free energy barrier is only 68.2 kJ·mol^{-1}, but the formation of *Para*-xylene (PX) needs to overcome a high barrier of 129.2 kJ·mol^{-1}. However, ZnOH$^+$/BAS−HZSM−5 exhibits relative high activity for the formation of methoxy with the Gibbs free energy barrier of 113.9 kJ·mol^{-1}, and 92.9 kJ·mol^{-1} for PX. Meanwhile, the formation of PX is easiest among three xylenes. Therefore, ZnOH$^+$/BAS−HZSM−5 can be as the promising catalyst for the preparation of PX during methylation of toluene with methanol.

1. Introduction

Para-xylene (PX) is an important raw material in the chemical industry, which is mainly used to produce terephthalic acid and dimethyl terephthalate, as the monomer of industrial polymers, they can further synthesize polyester fiber, resin, film, polyester paint, engineering plastics and so on [1,2]. PX can be produced by methanol to gasoline (MTG), steam cracking of naphtha and catalytic reforming, along with the abundant by-products also be engendered, such as benzene, toluene and other xylene isomers [3,4,5]. Thus a direct process is responsible to improve the selectivity to PX. Toluene is formed in excess and the methylation reaction can occur with methanol, which is an important chemical raw material comes from coal, natural gas and biomass broadly [6,7,8]. The high yield of PX can be gained in a single pass conversion of methanol. This means that the separation of PX from three kinds of xylenes with similar boiling points in physics (*para*-xylene (PX)−411.5 K, *meta*-xylene (MX)−412.3 K, *ortho*-xylene (OX)−417.6 K) will be relatively simplified in a cost-effective manner [9,10,11]. However, the high energy barrier of methoxy formation and the low selectivity to PX

are the main disadvantages of methylation.

HZSM−5 is the main catalyst used in the methylation process [12,13,14] due to its hydrophobicity, high thermal and hydrothermal stability and higher aromatization activity [15,16,17].The unique three-dimensional cross framework structure of HZSM−5 has space limitation on reactants, intermediates and products. However, it is difficult for the aromatics shape selective catalysis to PX from the mixture of xylene isomers [2].

In the perspective of intrinsic reaction, methoxy is the significant intermediate and its production will influence the subsequent methylation process. For promoting the formation of methoxy, Zuo et al.[11] used CO_2 and H_2 as the reactants to reduce the Gibbs free energy barrier of surface methoxy species formation in ZnZrO$_x$−ZSM−5 (ZZO−Z5) dual-functional catalysts at 633 K. However, methanol is used as raw material to produce methoxy, which will need to overcome the high energy barrier. Moreover, it is not conductive to the activity and selectivity to PX. So looking for a way to reduce the energy barrier of methoxy formation is essential when taking methanol as raw material. Acidity is a considerable factor affecting the reaction activity and products

selectivity in HZSM−5 [18]. In the experimental study, acidity of catalyst can be affected by different types of acid sites and modifying the catalyst with different metals. Zhang et al.[19] showed that most of the introduced Cd cations could exchange with protons of bridged hydroxyl groups of HZSM−5, resulting in the reduction of the number of Brønsted acid site (BAS) while the formation of the new Lewis acid site (LAS) in catalyst. With the increasing of Cd content, the concentration of strong acid site decreased. Further, the quantity of BAS decreased while the quantity of LAS increased, and the selectivity to PX increased. Niu et al. [20] found that HZSM−5 is modified by ZnOH$^+$, which would improve the dehydrogenation of light hydrocarbons and help to convert into aromatics. From the above results, it can be found that the acid types and strengths of BAS and LAS affect the distribution of aromatics and the selectivity to PX in HZSM−5 catalysts. Among them, BAS is mainly the framework bridged OH group, namely Si−OH−Al [21,22]. LAS is the extra-framework aluminum (EFAl) species, which is formed by the partial releasing of aluminum from the zeolite framework through mild hydrothermal/heat treatment [23,24,25], or LAS is formed by the proton exchanging of metal ions and bridged hydroxyl groups in the modification process [19]. However, the effect of LAS on the microscopic mechanism of methylation of methanol with toluene to xylenes has not been theoretically documented yet, so it is very important to study the effect of LAS/BAS to the *C−O* bond breaking of methanol and activity with selectivity to PX from the perspective of intrinsic reaction in HZSM−5.

In this study, Density Functional Theory (DFT) method will be used to explore the reaction path of methylation of methanol with toluene to xylenes in HZSM−5 with BAS and LAS/BAS, respectively. Through analyzing reaction pathway, Gibbs free energy barriers, Bader charge (*e*), the bond length (Å) and acid strength of catalysts to explore the synergistic effect of LAS/BAS, and its effect to the surface methoxy formation, the formation activity and selectivity to PX.

2. Calculation details

2.1. Calculation methods

All DFT calculations were carried out using the Vienna ab initio simulation package (VASP) program [26,27,28]. The generalized gradient approximation (GGA) method was used in combination with the Perdew-Burke-Ernzerhof (PBE) exchange-correlation functional [29]. The Projector Augmented Wave (PAW) method was used to describe the electron-ion interactions and the plane-wave cutoff energy at 400 eV (1 eV = 96.485 kJ·mol^{-1}). For further verifying the rationality of the plane-wave cutoff energy at 400 eV, the adsorption energies of CH$_3$OH in BAS-HZSM−5 catalyst were calculated with three different cutoff energies at 400, 450 and 500 eV. The relative structures and adsorption energies were listed in Table 1 and the Eqn. (1) of E_{ads} is:

$$E_{ads} = E_{total} - E_{CH_3OH} - E_{zeol} \qquad (1)$$

where E_{total}, E_{CH_3OH} and E_{zeol} referred to the total energy of CH$_3$OH and

BAS-HZSM−5, the energies of CH$_3$OH and BAS-HZSM−5, respectively. The results indicated that the largest difference of bond distance between the O atom of methanol and H proton was less than 0.041 Å, and the difference of adsorption energy was less than 3.8 kJ·mol^{-1} for three different cutoff energies. So the plane-wave cutoff energy at 400 eV was reasonable with a tiny difference. Further, a more accurate explanation was acquired at the website of 'The VASP Manual'. The default of ENCUT is the largest ENMAX on the POTCAR file, and the corresponding value is 400 eV in this work. Finally, the cutoff energy at 400 eV was determined from the parameter setting about zeolites in previous works. Demuth et al.[30] obtained the conclusion that the sterical constraints of zeolites would affect the energy barrier of trimethyldiphenylmethane intermediate formation by the disproportionation reaction of xylenes in 10- and 12-membered ring with a plane-wave cutoff of 400 eV. And Xu et al.[31] proved the composite Na/Fe and HZSM−5 catalyst showed high CO$_2$ conversion ability and leading to the relatively stable aromatics synthesis when the cutoff energy was at 400 eV. So the cutoff energy of 400 eV could adequately be used to calculate the properties of the catalysts in this work through three aspects of demonstration.

The Gaussian smearing method with the SIGMA value of 0.2 eV [32] and the spin polarized calculation was operated with the ISPIN value of 2 [33]. Γ-point mesh was used to sample the Brillouin zone for all zeolites. In previous works, Rozanska et al.[34] found steric constraints were strongly dependent on the transition-state structure as well as on the zeolite topology with a Brillouin zone sampling restricted to the Γ-point. Dai et al.[35] considered the Ga introduction can increase the selectivity to aromatics in HZSM−5 with the single Γ-point as the center. So the Brillouin zone sampling was restricted to the Γ-point, which is reasonable for HZSM−5 catalysts in this work. The force threshold of 0.05 eV·Å^{-1} (1 Å = 1 × 10^{-10} m) and the energy on each atom was converged to 1 × 10^{-5} eV were used for the structure optimization [17, 36].

The climbing-image nudged elastic band (CI-NEB) method combined with dimer method to find out the transition states (TSs) between reactants and products [31,36]. When the force threshold was less than or equal to 0.07 eV·Å^{-1}, the convergence criterion was reached [37]. The reaction energy (E_r) and the energy barrier (E_a) for every elementary step were derived from the following Eqn. (2) and (3), respectively.
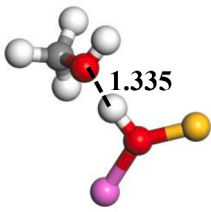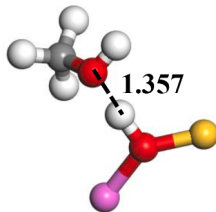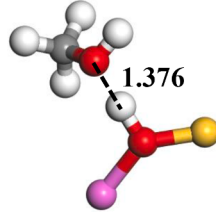
$$E_r = E_{FS} - E_{IS} \qquad (2)$$

$$E_a = E_{TS} - E_{IS} \qquad (3)$$

where E_{IS}, E_{FS} and E_{TS} referred to the total energies of the reactant, the product and the transition state in the elementary reaction, respectively.

The frequency calculations were employed in this work and the Gibbs free energies at 673 K were then calculated from frequencies. The experimental operating temperature of 673 K also was used to study and compare the reaction mechanism with kinetic performance of benzene ethylation by ethanol orethylene in H-ZSM-5, a conclusion of ethylene-involved reaction being hundreds of times higher than the ethanol-involved reaction was obtained [27]. Also McCann et al.[38] demonstrated the stable electrostatic confinement effect of zeolite framework,

Table 1

The bond distances (Å) and adsorption energies (kJ·mol^{-1}) of CH$_3$OH in BAS−HZSM−5 with the cutoff energies of 400, 450 and 500 eV.

ENCUT (eV)	400	450	500
Bond distance (Å)	1.335	1.357	1.376
E_{ads} (kJ·mol^{-1})	−63.3	−63.6	−67.1

which can effectively reduce the Gibbs free energy barriers of reactions with a same experimental operating temperature of 673 K.

2.2. Calculation models

HZSM−5 zeolite was represented by 46T cluster as the model catalyst. It was extracted from its crystallographic structural data [16,38, 39]. The terminal Si−H was oriented along the direction of the corresponding Si−O bond and the bond length was set to 1.470 Å [40]. The BAS was formed by substituting one silicon with an aluminum atom at T12 and the negative charge of −e was compensated by the H proton to forming the Al12−O(H)−Si3, which was located at the intersection of straight and sinusoidal channels, provided the largest reaction space and beneficial to the aromatization reaction [5,41,42,43]. The LAS was formed by extra-framework aluminum hydroxyl group (AlOH^{2+}), which located in the 6-membered ring of cavity and stable with the adjacent BAS in AlOH^{2+}/BAS−HZSM−5 [40]. In order to ensure the electrical neutrality of AlOH^{2+}/BAS−HZSM−5, two framework Si atoms were replaced by Al atoms and separated by two framework Si atoms in calculated models [44,45,46]. The stoichiometric number were $Si_{45}Al_1O_{68}H_{49}$ for BAS−HZSM−5 and $Si_{43}Al_4O_{69}H_{50}$ for AlOH^{2+}/BAS−HZSM−5 in this work and the computational models were shown in Fig. 1. The Al atom and the adjacent $HOSiO_3(SiO_4)_3$ that responsible to the reaction were relaxed, and the other atoms were fixed for BAS−HZSM−5. For AlOH^{2+}/BAS−HZSM−5, the $O_3SiO(H)Al(OSiO_3)_3$, the 6-membered ring with AlOH^{2+} and two substituted Al atoms were relaxed, the other atoms were fixed. For the modification model with ZnOH$^+$, the ZnOH$^+$ was situated near BAS and located in the 5-membered ring of the straight channel to providing better catalytic activity [47,48]. For ensuring the electrical neutrality of ZnOH$^+$/BAS−HZSM−5 and stabilizing the ZnOH$^+$, a silicon atom was replaced by an aluminum atom with the order of Al−O(H)−Si−O−Al at the 5-membered ring. In this model, the $O_3SiO(H)Al(OSiO_3)_3$ and the 5-membered ring with ZnOH$^+$ were relaxed, the other atoms were fixed.

The active site locations of BAS, AlOH^{2+} and ZnOH$^+$ were same with literature data from the Table 2. The BAS was usually located in Al12−O (H)−Si3 of HZSM−5 for MTA reaction. Wen et al.[41] indicated that the carbocations of $C_7H_9^+$-$C_{12}H_{19}^+$ were important intermediates, and methane was formed via intramolecular hydrogen transfer reaction in MTA process with the active site of Al12−O(H)−Si3 as BAS. The Gibbs free energy barrier of alkylation with benzene by ethene over HZSM−5 agreed with experimental data (58–76 kJ·mol^{-1}) with the same BAS of Al12−O(H)−Si3 at 653 K [42]. For the AlOH^{2+}/BAS−HZSM−5, the active site location of AlOH^{2+} was 6-membered ring of cavity and stable with the adjacent BAS in HZSM−5 catalyst. This location was in line with the structure of 72T-HZSM−5, which was used to the initial carbon–carbon (C–C) bond formation in methanol-to-olefin (MTO) reaction by a new methane–formaldehyde pathway, also with extra-framework AlOH^{2+} located in same site and stable with the adjacent BAS in HZSM−5 zeolite [40]. Similarly, the ZnOH$^+$ location was 5-membered ring of the straight channel for ZnOH$^+$/BAS−HZSM−5, this structure was used to study the effect of abundant H$_2$ on ethylene aromatization, and a conclusion of the amount of ZnOH$^+$ species was increased after H$_2$ pretreatment, which further increased the selectivity to aromatics [47]. In addition, the deprotonation energies (DPE) of BAS−HZSM−5, AlOH^{2+}/BAS−HZSM−5, ZnOH$^+$/BAS−HZSM−5 were in line with the DPE values of 1205–1414 kJ·mol^{-1} in the literature data [49]. Montejo-Valencia et al. [50] also demonstrated that the formation of open sites through the hydrolysis of MFI was not energetically favorable with the DPE value of 1200 to 1250 kJ·mol^{-1} for Al−MFI zeolites. So
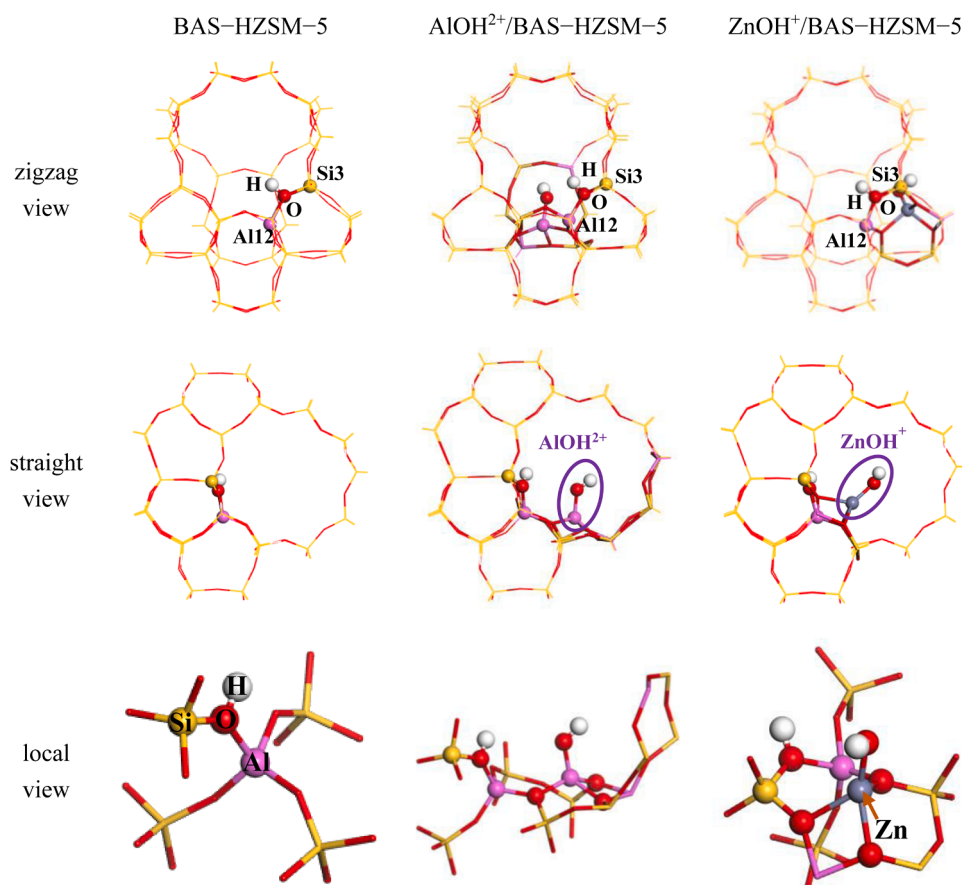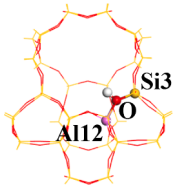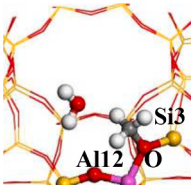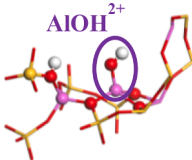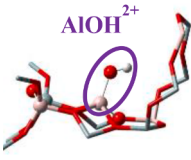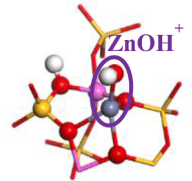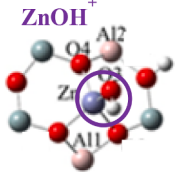

Fig. 1. The calculated models for BAS−HZSM−5, AlOH^{2+}/BAS−HZSM−5 and ZnOH$^+$/BAS−HZSM−5 with the perspective of zigzag view, straight view and local view.

Table 2
The location and the deprotonation energies (kJ·mol^{-1}) for BAS−HZSM−5, AlOH^{2+}/BAS−HZSM−5 and ZnOH^{+}/BAS−HZSM−5 catalysts constructed in this work and reference.

catalysts	location this work	reference	deprotonation energy (DPE) this work	reference
BAS−HZSM−5			1282.4	1205−1414
AlOH^{2+}/BAS−HZSM−5			1192.8	1205−1414
ZnOH^{+}/BAS−HZSM−5			1272.4	1205−1414

through the above analysis, it can be sure that three catalyst models constructed in this work were rational.

3. Results and discussion

3.1. The reliability of model

The route of methanol and toluene are used as raw materials to produce xylenes can be divided into the concerted pathway and the stepwise pathway. The formation of methoxy is the crux to distinguish two pathways. According to the previous work, the rate-determining step of stepwise pathway was methoxy formation and the Gibbs free energy barrier of this step was 145.0 kJ·mol^{-1} at 673 K. However, the methyl group in methanol attacked the *para, meta* and *ortho* carbons of toluene to produce the $C_8H_{11}^{+}$ intermediates, which was the rate-determining step of the concerted pathway. And the Gibbs free energy barriers of PX, MX and OX formation were 167.0, 138.0 and 139.0 kJ·mol^{-1} at 673 K, respectively [1]. It can be known that the stepwise pathway is slightly better than the concerted pathway by comparing the rate-determining step barriers of PX production in two pathways. Also Wang et al.[27] found that the stepwise mechanism was the crux to govern the activity of ethanol-involved reaction. So the stepwise pathway of xylenes formation with methanol and toluene in BAS−HZSM−5 is studied in this work and the reaction route is shown in Scheme 1. In this path map, 'Z' represents the zeolite, which is different HZSM−5 catalysts in this work. 'ZOH' and 'ZOCH$_3$' special refer to the HZSM−5 catalysts with H protons and methoxy, respectively. 'ZO^{-}' expresses the zeolites without H protons.

The 46T and 72T models of BAS−HZSM−5 are chosen for methoxy formation because they can visually represent the localization of transition state, reasonably describe the space constraint and electrostatic stability effect of molecular sieve skeleton, which is vital to the quantitative description of aromatics selectivity [39,47,51,52]. The reaction Gibbs free energy profile for the production of methoxy in 46T and 72T is shown in Fig. 2. The first step of this pathway is the formation of methoxy, and it involves the initial adsorption of methanol. Methanol is absorbed in a side-on adsorption mode on BAS and positioned parallel to the pore walls. The O atom of CH$_3$OH is directed towards the acid site and there is only one strong hydrogen bond with the distance of 1.335 Å
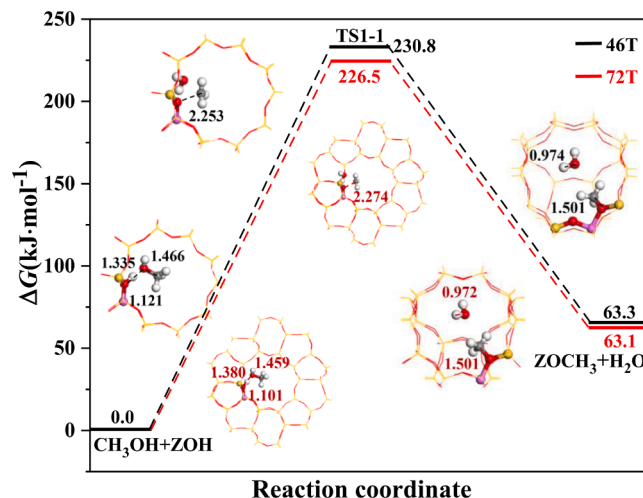
Fig. 2. The reaction Gibbs free energy profile and the reactants, transition states (TS) and products structures about the formation of methoxy in BAS−HZSM−5 with 46T and 72T at 673 K.

in 46T and 1.380 Å in 72T. The formation of methoxy by methanol is displayed in Fig. 2, the H proton is combined with the O atom of methanol, the distances of the H−O bonds being broken are 1.121 and 1.101 Å in the 46T and 72T, and the new formed H−O bonds are 0.974 Å in the 46T and 0.972 Å in the 72T. The C−O bonds of methanol are broken with 1.466 and 1.459 Å at once in 46T and 72T, and the new C−O bonds are formed with the same bond distance of 1.501 Å. The water molecule is adsorbed around methoxy group. In the transition state structure, the distance between the planar methyl C atom and the O atom of BAS is 2.253 Å with a Gibbs free energy barrier of 230.8 kJ·mol^{-1} in 46T, also the corresponding distance is 2.274 Å and the Gibbs free energy barrier is 226.5 kJ·mol^{-1} in 72T. The structures and Gibbs free energy barriers of methanol dehydration in 46T model are almost in line with the results of 72T model. Also they are consistent with the Andzelm's [53] result (226.1 kJ·mol^{-1}) in Ferrierite, which contains 54 atoms and Zicovichwilson's [54] result (217.7 kJ·mol^{-1})

obtained in $H_3SiOHAlH_2OSiH_3$ model of H-zeolite, respectively. Moreover, the 46T cluster as the HZSM−5 model catalyst have been used for abundant works. McCann et al.[38] considered the 46T cluster as the full-cage representation of the HZSM−5 zeolite, which can be used to Methanol-to-Olefin (MTO) conversion. Speybroeck et al.[39] had the same view, which was the location of transition states and interpretation of the normal modes being substantially simpler in 46T finite HZSM−5 zeolite cluster than the periodic approach from a computational technical point of view, and a conclusion of the absolute reaction rates can be calculated with near chemical accuracy was obtained. All these examples demonstrate that the size of model has no obvious effect on the structures and Gibbs free energy barriers of the reaction, and then explains the 46T cluster as the HZSM−5 model catalyst is appropriate for this work. The water molecule will not react with the species in the subsequent process, so it can be considered that the water molecule is desorbed in the following step.

3.2. The production of xylenes in BAS−HZSM−5

Then the toluene molecules enter the 10-member ring pore of HZSM−5 and are separately adsorbed on the location near methoxy with the *para, meta* and *ortho* sites. The relative distances between the methyl carbon and the ring carbon of *para, meta* and *ortho* sites are 3.211, 3.443 and 3.490 Å, respectively. In the next step, the methyl attacks the *para, meta* and *ortho* sites of toluene to form the $C_8H_{11}^+$ intermediate. The correlative structures of reactants, transition states (TS) and products of this step are shown in Fig. 3. According to the TS structures, the methyl groups are almost planar and parallel to toluene molecules. The C−O bonds are broken with 2.082, 2.125 and 2.154 Å and the C−C bonds are formed with 2.258, 2.253 and 2.296 Å in *p*-TS1–2, *m*-TS1–2 and *o*-TS1–2, respectively. The Gibbs free energy barriers for the formation of *p*-$C_8H_{11}^+$−1, *m*-$C_8H_{11}^+$−1 and *o*-$C_8H_{11}^+$−1 are 66.2, 81.5 and 90.9 kJ·mol^{-1}.

After the C_8H_{11} intermediates formation, they are adsorbed at the cross channels of HZSM−5 and the methyl groups are toward the BAS. For PX, MX and OX production, which need to back-donate the H proton to the framework oxygen. So the C_8H_{11} intermediates are rotated and be marked as *p*-rot1, *m*-rot1 and *o*-rot1 (Fig. 3). The rotation Gibbs free energies are 2.3, 37.6 and −25.4 kJ·mol^{-1} for *p*-rot1, *m*-rot1 and *o*-rot1 formation, respectively. The H−C bonds are broken with 1.354, 1.361 and 1.404 Å and the H−O bonds are formed with 1.384, 1.375 and 1.309 Å according to the TS structures about PX, MX and OX formation, respectively. The corresponding Gibbs free energy barriers are 4.6, 6.5 and 38.9 kJ·mol^{-1} at 673 K.

The methylation reaction in BAS−HZSM−5 catalyst have been completed in this work. In order to facilitate the methylation process in different HZSM−5 catalysts smoothly, the accuracy rationality of 0.07 eV·Å^{-1} in the transition state search process is verified. And different elementary reaction are selected, which are proton transfer for PX formation and the formation of $C_8H_{11}^+$ intermediate for OX formation. The
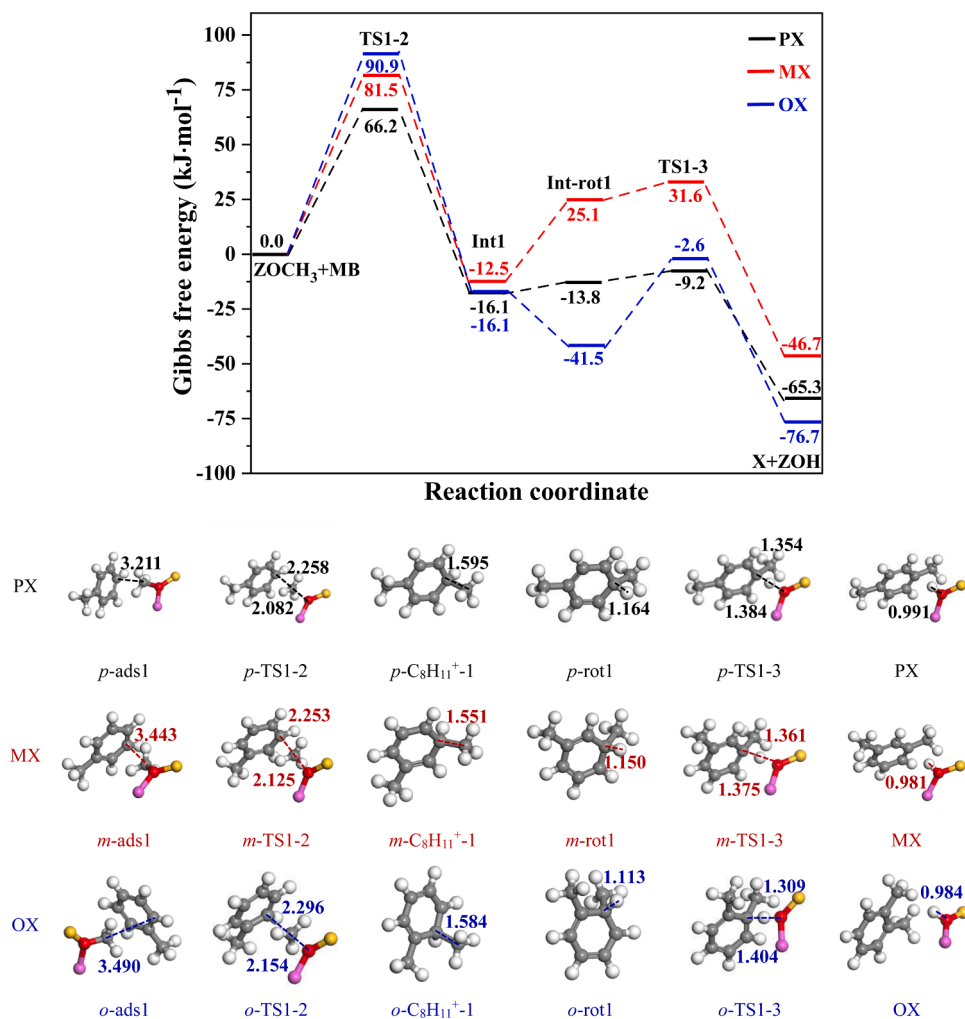

Fig. 3. The reaction Gibbs free energy profile and the reactants, transition states (TS) and products structures about the formation of PX, MX and OX in BAS−HZSM−5 at 673 K.

relative Gibbs free energy barriers and transition state structures are listed in Table 3. The Gibbs free energy barriers for proton transfer leading to the formation of PX are 6.5 and 4.6 kJ·mol^{-1} with the force convergence accuracies of 0.05 and 0.07 eV·Å^{-1}, respectively. The corresponding difference of Gibbs free energy barriers is only 1.9 kJ·mol^{-1}, and the transition state structures are same. In addition, the formation of $C_8H_{11}^+$ intermediate for OX formation is also studied with the force convergence accuracies of 0.05 and 0.07 eV·Å^{-1}, there is only a small difference for Gibbs free energy barrier with 0.6 kJ·mol^{-1} and the difference is less than 0.008 Å for bond lengths. Therefore, the Gibbs free energy barriers and the corresponding structures in the transition state search process can be correctly reflected when the force threshold is 0.07 eV·Å^{-1} in this work. And Vos et al.[37] studied the alkylation reaction of toluene with methanol catalyzed by the acidic Mordenite (Si/Al = 23) with the force threshold of 0.07 eV·Å^{-1}, and a conclusion of the steric constraint energy contribution having a significant effect on the energies and bond formation paths was obtained. So the force threshold of 0.07 eV·Å^{-1} was reasonable for this system, and it can ensure the comparability of the calculation results.

It can be seen that the rate-determining step of xylenes production in BAS−HZSM−5 is methanol dissociation and the corresponding Gibbs free energy barrier is 230.8 kJ·mol^{-1}, it is too high to be conductive to the formation of methoxy, therefore is unfavorable for generating xylenes. By understanding the previous work, the releasing of aluminum from a zeolite framework would cause the EFAl species formation in a mild hydrothermal/thermal treatment. Also Chen et al.[55] proved that the BAS and the extra-framework Al–OH species were adjacent by a synergistic effect existed in LAS and the adjacent BAS, along with using the 2D exchange NMR experiment. Moreover, the synergistic effect of LAS/BAS was proved in the methane-formaldehyde mechanism route, which differs from the traditional pathway at the isolated BAS [40]. In addition, the synergistic effect of LAS/BAS could promote the selectivity to aromatic compounds [19]. So in the next part of the study, the influence of LAS to the generation route, activity and selectivity to xylenes will be considered.

3.3. The formation of xylenes in AlOH^{2+}/BAS−HZSM−5

According to the previous work, a possible mechanism route about the methylation to xylenes at LAS/BAS is proposed by considering the synergy effect, which is differs from the route at the isolated BAS. The reaction route is shown in Scheme 2.

The reaction Gibbs free energy profile for the production of xylenes is shown in Fig. 4 and the reactants, transition states and products structures about the formation of PX, MX and OX in AlOH^{2+}/BAS−HZSM−5 are displayed in the Fig. S1. The first step of this pathway is also the formation of methoxy. The methanol is absorbed in a side-on adsorption mode on BAS and the H proton has a bond with methanol to form $CH_3OH_2^+$ intermediate after optimization. The O···H−O intermolecular distance is 2.508 Å. It is different from the above situation of methyl group having a bond with framework O atom, the methyl C atom is
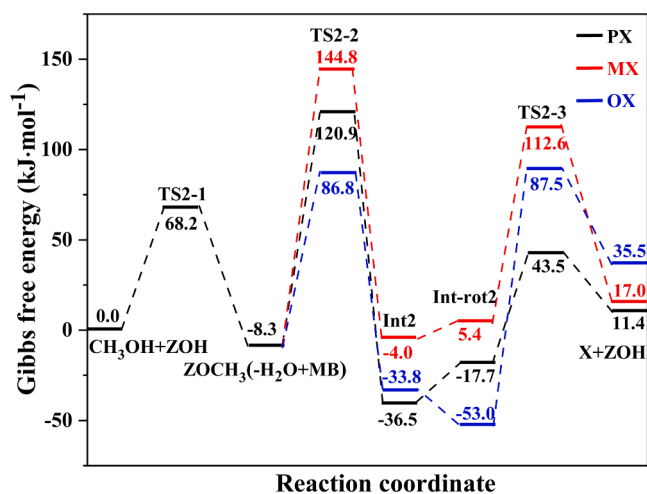

Fig. 4. The reaction Gibbs free energy profile for the production of xylenes in AlOH^{2+}/BAS−HZSM−5 at 673 K.

combined with O atom of AlOH^{2+} and the corresponding methoxy is formed in the methanol dissociation process. From the TS structure, it can be seen that the O atom of water molecule, the C atom of methyl and the O atom of AlOH^{2+} is almost in a straight line and the methyl is almost planar. The length between the O of water molecule and the C of methyl is 1.969 Å and a distance of 1.978 Å between the C of methyl and the O of AlOH^{2+}. The corresponding Gibbs free energy barrier of this step is 68.2 kJ·mol^{-1}. Similar to the situation of the above study, the water molecule is desorbed in the following step, because it will not participate in the following reaction.

Next, the process of production to the $C_8H_{11}^+$ intermediates and the final xylenes is nearly identical with the corresponding process in BAS−HZSM−5. So a brief description about this process in LAS/BAS is given. The toluene molecules enter the intersection of zeolite and are adsorbed around the methyl group. From the reactants structures in the Fig. S1, it can be seen that the methyl groups are not oriented to the *para*, *meta* and *ortho* sites of ring carbon of toluene after structural optimization, this is due to the repulsive effect existing in the methyl and toluene when the methyl is situated above the AlOH^{2+}. In the TS structures, the methyl is almost planar and situates in the middle of AlOH^{2+} and toluene. The distances between the O atom and the methyl C atom are 2.131, 2.280 and 2.067 Å, and the C−C bonds lengths are 2.278, 2.538 and 2.222 Å for the *p*-$C_8H_{11}^+$−2, *m*-$C_8H_{11}^+$−2 and *o*-$C_8H_{11}^+$−2, respectively. The corresponding Gibbs free energy barriers are 129.2, 153.1 and 95.1 kJ·mol^{-1}.

For back-donating the H proton to the framework oxygen to form complete BAS and the final products, the $C_8H_{11}^+$ must be rotated. The rotation Gibbs free energies are 18.8, 9.4 and −19.2 kJ·mol^{-1} for the formation of *p*-rot2, *m*-rot2 and *o*-rot2, respectively. The result illustrates that the production of *o*-rot2 is an exothermic process. For the last

Table 3
The Gibbs free energy barriers (kJ·mol^{-1}) and the transition state structures (Å) about proton transfer for PX formation and the formation of $C_8H_{11}^+$ intermediate for OX formation with differentforce threshold of 0.05 and 0.07 eV·Å^{-1} in BAS−HZSM−5 at 673 K.

Reaction	PX-TS1−3		OX-TS1−2	
Accuracy (eV·Å^{-1})	0.05	0.07	0.05	0.07
ΔG_a (kJ·mol^{-1})	6.5	4.6	91.5	90.9
Bond length (Å)	1.354 / 1.384	1.354 / 1.384	2.293 / 2.146	2.296 / 2.154

step of final xylenes formation, the Gibbs free energy barriers are 61.2, 107.2 and 140.5 kJ·mol^{-1} for PX, MX and OX, and BAS is formed on the Si12-O(H)-Al12 for OX, which is differs from the situation of Al12−O (H)−Si3 as the site of BAS formation. This is due to the H proton on Si12-O-Al12 site is more stable than Al12−O−Si3 site for the formation of OX in AlOH^{2+}/BAS−HZSM−5.

By comparing the results of xylenes formation in BAS−HZSM−5 and AlOH^{2+}/BAS−HZSM−5, it can be known that AlOH^{2+}/BAS−HZSM−5 shows the better activity and selectivity to PX than BAS−HZSM−5. This shows that the synergistic effect of LAS/BAS is instrumental in the dissociation of methanol and the methylation reaction of methanol and toluene. According to previous works, the modification to HZSM−5 with Zn could improve the selectivity to aromatics. The results of Yu et al. [56] demonstrated that the product distribution content of PX increase with the raising of Zn. Moreover, most of Zn existed as ZnOH$^+$ species when they are introduced into zeolite, and ZnOH$^+$ could restrain the side reactions of methanol in order to accelerate the alkylation of benzene and methanol [57]. In addition, ZnOH$^+$ species helped accelerate the aromatization by acting as dehydrogenation site [47]. So in the next section, a modification to HZSM−5 with ZnOH$^+$ species and the effect on the activity and selectivity to PX will be discussed.

3.4. Methylation of toluene with methanol in ZnOH$^+$/BAS−HZSM−5

The mechanism route about methylation in ZnOH$^+$/BAS−HZSM−5 is the same as that in AlOH^{2+}/BAS−HZSM−5. The reaction Gibbs free energy profile for the production of xylenes is shown in Fig. S2. Owing to the methyl will be located on the ZnOH$^+$ to form methoxy, the methyl of

methanol faces to the ZnOH$^+$ and the methanol is adsorbed in the end-on mode (Fig. 5), which is different from the adsorption mode on the BAS and AlOH^{2+}/BAS. There are two hydrogen bonds with lengths of 1.175 Å between the O atom of methanol and the H proton of HZSM−5, and the distance of 2.072 Å between the H atom of methanol and the framework O atom of Si12-O-Al12. The CH$_3$OH has a bond with the H proton of BAS and this process is same with the formation of CH$_3$OH$_2^+$ intermediate on the AlOH^{2+}/BAS. In the TS structure of the methoxy formation, the O atom of H$_2$O, the C atom of methyl and the O of ZnOH$^+$ are almost in the line and this result is in accordance with the AlOH^{2+}/BAS. The methyl is planar and the Gibbs free energy barrier is 113.9 kJ·mol^{-1}, which is lower than the Gibbs free energy barrier of methanol dissociation in BAS−HZSM−5 (230.8 kJ·mol^{-1}) and higher than corresponding energy in AlOH^{2+}/ BAS−HZSM−5 (68.2 kJ·mol^{-1}).

Toluene enters the intersection of zeolite and methyl group orients to the *para, meta* and *ortho* sites of toluene to further forming the C$_8$H$_{11}^+$ intermediate. The Gibbs free energy barriers for the formation of the *p*-C$_8$H$_{11}$−3, *m*-C$_8$H$_{11}$−3 and *o*-C$_8$H$_{11}$−3 are 92.9, 133.6 and 109.4 kJ·mol^{-1} and the C−C bonds lengths are 1.599, 1.676 and 1.640 Å for the *para, meta* and *ortho* sites in the TS structures, respectively. It is similar to the route of the new BAS and final xylenes formation in BAS−HZSM−5 and AlOH^{2+}/BAS−HZSM−5, the C$_8$H$_{11}$ intermediates need to be rotated and the rotation Gibbs free energies are 10.6, −14.2 and −13.7 kJ·mol^{-1} for *p*-rot3, *m*-rot3 and *o*-rot3 formation, and this result means that the rotation of *p*-C$_8$H$_{11}^+$−3 is a endothermic reaction. Finally, the H proton of the C$_8$H$_{11}$ intermediate orients to the framework oxygen which is included in the original BAS, and then attacks it to form final xylenes. The Gibbs free energy barriers are 55.8, 20.3 and 54.6

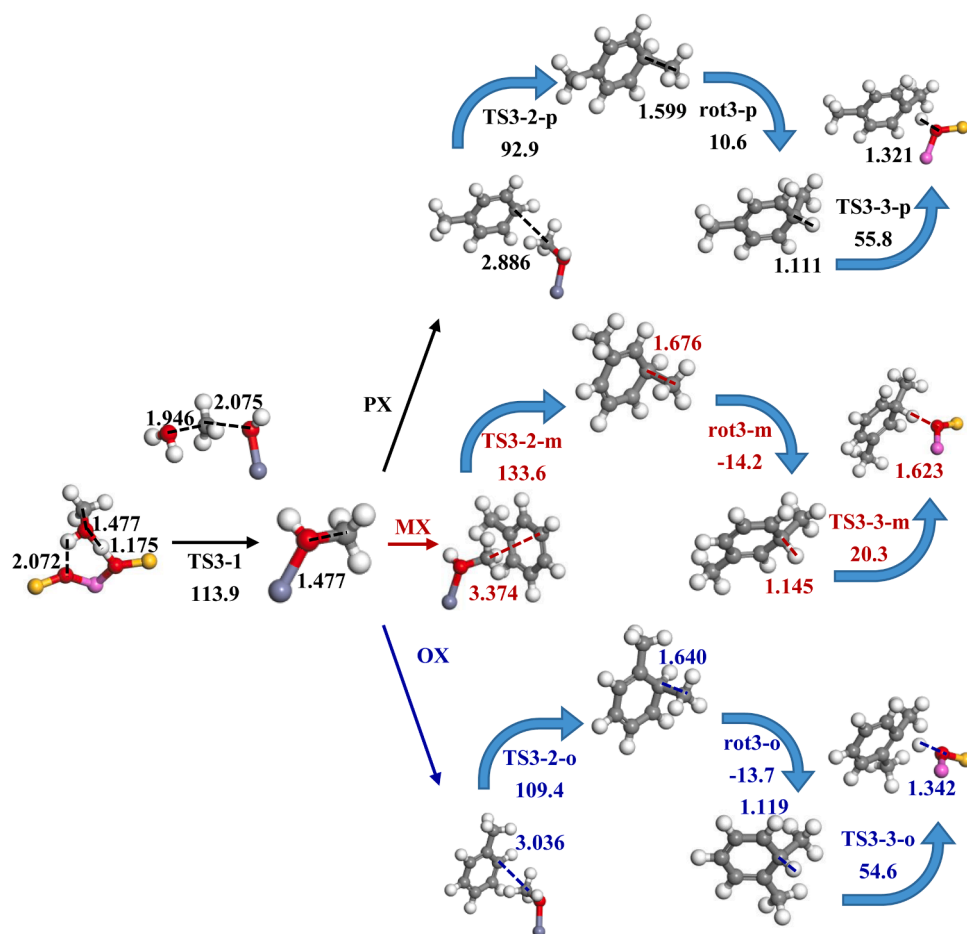**Fig. 5.** The Gibbs free energy barriers (kJ·mol^{-1}) and reaction Gibbs free energy for the rotation steps (kJ·mol^{-1}), as well as the reactants, transition states (TS) and products structures for the production of xylenes in ZnOH$^+$/BAS−HZSM−5 at 673 K.

kJ·mol⁻¹ for PX, MX and OX production, respectively.

3.5. General discussion

From above study, it can be known that the production of xylenes with methanol and toluene can be divided into the formation of methoxy and the methylation process.

3.5.1. The analysis of methoxy formation

The formation routes of methoxy are different in BAS−HZSM−5 and LAS/BAS−HZSM−5. From the Fig. 6, it can be known that the distinguish is LAS catalyzes the formation of methoxy and the methyl has a bond with the O atom of LAS in AlOH²⁺/BAS−HZSM−5 and ZnOH⁺/BAS−HZSM−5 compared to BAS−HZSM−5. This result illustrates that the synergistic effect of LAS/BAS firstly manifests the participation of LAS and BAS in methoxy formation and producing a pathway which differs from that on the isolated BAS. And it is in line with the result that LAS could act as an active center to participating in the acid-catalyzed reaction, and it is distinct from Brønsted acid catalysis [58,59].

Besides the pathways, there is also a big difference between BAS−HZSM−5 and LAS/BAS−HZSM−5 for the Gibbs free energy barriers of methoxy formation. By comparing Gibbs free energy barriers of methanol dissociation in BAS−HZSM−5 (230.8 kJ·mol⁻¹), AlOH²⁺/BAS−HZSM−5 (68.2 kJ·mol⁻¹) and ZnOH⁺/BAS−HZSM−5 (113.9 kJ·mol⁻¹), it can be found the synergistic effect of LAS/BAS is profit to produce methoxy. Moreover, the C−O bond breaking of dimethyl ether (DME) would produce the Gibbs free energy barrier of 179.6 kJ·mol⁻¹ when there was only BAS [60]. However, the Gibbs free energy barrier reduced to 149.9 kJ·mol⁻¹ for the C−O bond breaking of DME when BAS and LAS existed at the same time [40]. So the effect of the synergistic effect of LAS/BAS to methanol dissociation should be studied.

In here, the relationships among the synergistic effect of LAS/BAS, the Gibbs free energy barriers, the Bader charges (e) and the bond lengths (Å) are analyzed for methoxy formation in BAS−HZSM−5, AlOH²⁺/BAS−HZSM−5 and ZnOH⁺/BAS−HZSM−5. As shown in Table 4, Q_C means the Bader charges at the C atom of the methyl in the TS structures for methoxy formation. And the corresponding Q_C are 0.16, −0.04 and 0.09 e in BAS−HZSM−5, AlOH²⁺/BAS−HZSM−5 and ZnOH⁺/BAS−HZSM−5, respectively. Firstly, it can be known that the more easily methoxy is formed with the decreasing of Bader charges by contrasting the Gibbs free energy barriers and Q_C. Also the synergistic effect of LAS/BAS in AlOH²⁺/BAS−HZSM−5 and ZnOH⁺/BAS−HZSM−5 causes Q_C to reduce, and further improves the activity of methoxy formation compared to BAS−HZSM−5. Importantly, methoxy is more easily formed in the case of electron losing in contrast to electron accepting, so AlOH²⁺/BAS−HZSM−5 with Q_C of −0.04 e shows the highest activity with the Gibbs free energy barrier of 68.2 kJ·mol⁻¹ for methoxy formation. Besides Q_C, the bond distances between methanol C atom and active site O atom in the TS structures of methoxy formation

Table 4
The Gibbs free energy barriers (kJ·mol⁻¹), the Bader charges (e), the bond distances (Å) for methoxy formation, and the acid strengths (kJ·mol⁻¹) of BAS and LAS for BAS−HZSM−5, AlOH²⁺/BAS−HZSM−5 and ZnOH⁺/BAS−HZSM−5[a].

	BAS−HZSM−5	AlOH²⁺/ BAS−HZSM−5	ZnOH⁺/ BAS−HZSM−5
ΔG_a (kJ·mol⁻¹)	230.8	68.2	113.9
Q_C(e)	0.16	−0.04	0.09
$D_{C−O}$ (Å)	2.253	1.978	2.075
BAS/DPE (kJ·mol⁻¹)	1282.4	1192.8	1272.4
LAS/BE (kJ·mol⁻¹)		127.8	52.6

[a] The ΔG_a(kJ·mol⁻¹) is the Gibbs free energy barriers (kJ·mol⁻¹) of methoxy formation, the Q_C(e) is the Bader charges at the C atom of the methyl in the TS structures for methoxy formation, the $D_{C−O}$ (Å) is the bond distances between the methyl C and the active site O in the TS structures of methoxy formation, the BAS/DPE (kJ·mol⁻¹) is acid strengths (kJ·mol⁻¹) of BAS and LAS/BE (kJ·mol⁻¹) is acid strengths of LAS for BAS−HZSM−5, AlOH²⁺/BAS−HZSM−5 and ZnOH⁺/BAS−HZSM−5.

are also analyzed and marked as $D_{C−O}$. And the corresponding distances are 2.253, 1.978 and 2.075 Å in BAS−HZSM−5, AlOH²⁺/BAS−HZSM−5 and ZnOH⁺/BAS−HZSM−5. It can be known that the synergistic effect of LAS/BAS reduces $D_{C−O}$ compared to the isolated BAS. Also Gibbs free energy barriers decrease with the bond distances shortening for methoxy formation in BAS−HZSM−5, ZnOH⁺/BAS−HZSM−5 and AlOH²⁺/BAS−HZSM−5 by contrasting the Gibbs free energy barriers and $D_{C−O}$. Similarly, AlOH²⁺/BAS−HZSM−5 with the shortest $D_{C−O}$ shows the highest activity for methoxy formation. So the synergistic effect of LAS/BAS not only changes methoxy formation pathway but also is friendly to the formation of methoxy by reducing Q_C and shortening $D_{C−O}$. Moreover, the least Gibbs free energy barrier for methoxy formation appears in AlOH²⁺/BAS−HZSM−5 with the minimum Q_C and $D_{C−O}$. Because more methoxy formation will provide more raw materials for the subsequent methylation process, BAS−HZSM−5 is not a suitable catalyst for the subsequent methylation process of methoxy and toluene to xylenes.

3.5.2. The analysis of the methylation process

The formed methoxy will attack the para, meta and ortho sites of ring carbon of toluenes to form the $C_8H_{11}^+$ intermediates, and further forming the corresponding xylenes in BAS−HZSM−5, AlOH²⁺/BAS−HZSM−5 and ZnOH⁺/BAS−HZSM−5 catalysts. And the comparison of methylation reaction in three catalysts is expressed in Fig. 7. For the methylation process, the Gibbs free energy barrier of PX formation is 66.2 kJ·mol⁻¹, and which are 81.5 and 90.9 kJ·mol⁻¹ for MX and OX in BAS−HZSM−5. This shows that the activity to PX is higher than MX and OX, also the selectivity to PX is higher than MX and OX with the Gibbs free energy barrier differences of 15.3 kJ·mol⁻¹ between PX and MX and 24.7 kJ·mol⁻¹ between PX and OX in BAS−HZSM−5. Similarly, the
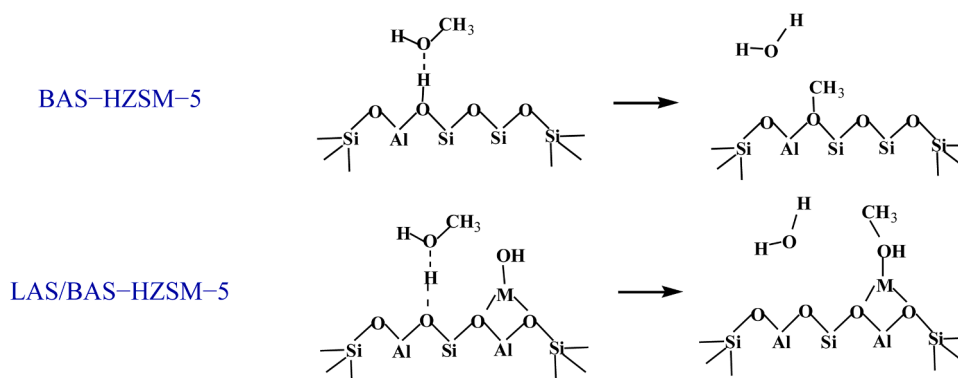
Fig. 6. The formation pathways of methoxy in BAS−HZSM−5 and LAS/BAS−HZSM−5. 'M' represents the different metals of LAS.
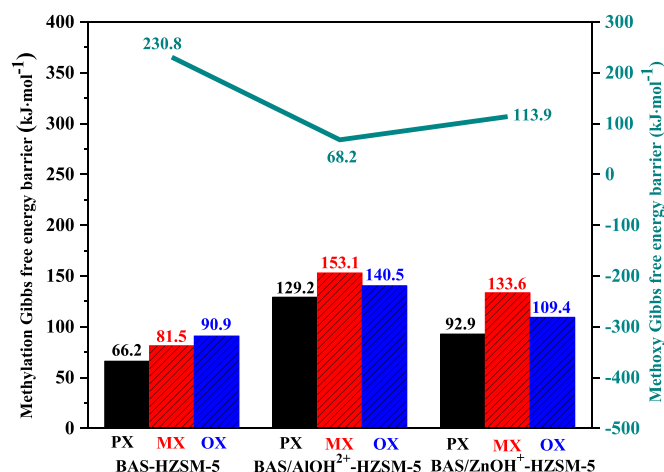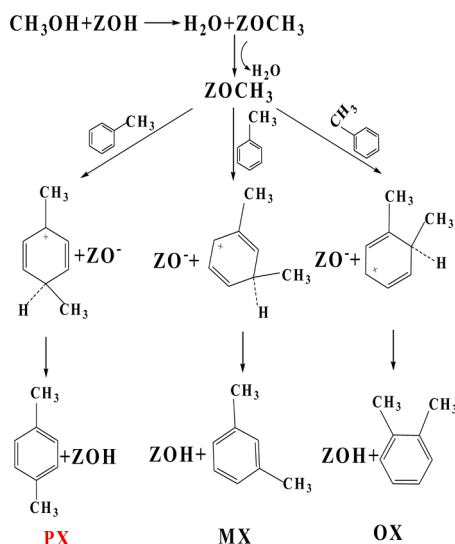
Fig. 7. The reaction Gibbs free energy barrier (kJ·mol^{-1}) for methoxy formation and the methylation process in BAS−HZSM−5, AlOH^{2+}/BAS−HZSM−5 and ZnOH^{+}/BAS−HZSM−5 at 673 K.

Scheme 1. The reaction route of methylation of toluene with methanol to xylenes in BAS−HZSM−5.

Gibbs free energy barrier of PX formation are all lower than MX and OX in AlOH^{2+}/BAS−HZSM−5 and ZnOH^{+}/BAS−HZSM−5 catalysts, and the activity to PX are higher than MX and OX in these two catalysts. At the same time, the selectivity to PX is higher than MX and OX with the Gibbs free energy barrier differences of 23.9 kJ·mol^{-1} in AlOH^{2+}/BAS−HZSM−5 and 40.7 kJ·mol^{-1} in ZnOH^{+}/BAS−HZSM−5 between PX and MX, also 11.3 kJ·mol^{-1} in AlOH^{2+}/BAS−HZSM−5 and 16.5 kJ·mol^{-1} in ZnOH^{+}/BAS−HZSM−5 between PX and OX. So it can be known that the activity and selectivity to PX are all better than MX and OX in three catalysts [19,47].

Combined with the above analysis of the activity to the methoxy formation in three catalysts, the highest Gibbs free energy barrier of 230.8 kJ·mol^{-1} for methoxy formation in BAS−HZSM−5 catalyst is not conductive to the methylation reaction of methoxy with toluene, also which is not beneficial to the formation of PX. However, it shows the preferable activity to the dissociation of methanol in AlOH^{2+}/BAS−HZSM−5 and ZnOH^{+}/BAS−HZSM−5 catalysts. Further comparing the Gibbs free energy barriers to PX formation with 129.2 and 92.9 kJ·mol^{-1} in AlOH^{2+}/BAS−HZSM−5 and ZnOH^{+}/BAS−HZSM−5 catalysts, it can be found that the activity to PX formation in ZnOH^{+}/BAS−HZSM−5 is better than AlOH^{2+}/BAS−HZSM−5.

So ZnOH^{+}/BAS−HZSM−5 is better for the formation to PX than AlOH^{2+}/BAS−HZSM−5 and BAS−HZSM−5 [61,62].

3.5.3. The influence of acid type and acid strength to the methylation reaction

For further explaining the synergistic effect of LAS/BAS, the acid strengths of BAS and LAS are determined. Also the influence of different acid types and acid strengths to methoxy and PX formation are discussed in BAS−HZSM−5, AlOH^{2+}/BAS−HZSM−5 and ZnOH^{+}/BAS−HZSM−5 catalysts.

Firstly, the acid strengths of BAS are determined with the deprotonation energy (DPE), and LAS with the binding energy (BE) of trimethylphosphine (TMP) by the coordination of the P atom (on the TMP probe molecule) and the Lewis acid center [63,64]. The calculation formulas are as follow:

$$DPE = E_{H^+} + E_{A^-} - E_{HA} \tag{4}$$

$$BE = E_{Lewisacid} + E_{TMP} - E_{TMP-Lewisacid} \tag{5}$$

The E_{HA} and E_{A^-} are the energies of the protonated and deprotonated structures, separately. E_{H^+} is the energy of H proton. And the smaller of the absolute value of DPE, the easier the proton transferring and the stronger BAS acid strength. The $E_{Lewis\ acid}$, E_{TMP} and $E_{TMP\text{-}Lewis\ acid}$ represent the energies of Lewis acid structures, the isolated TMP and TMP-Lewis acid complexes. The higher of BE, the stronger LAS acid strength. And the values of DPE and BE are listed in the Table 4. The values of DPE are 1282.4, 1192.8 and 1272.4 kJ·mol^{-1} in BAS−HZSM−5, AlOH^{2+}/BAS−HZSM−5 and ZnOH^{+}/BAS−HZSM−5, and the BE are 127.8 and 52.6 kJ·mol^{-1} in AlOH^{2+}/BAS−HZSM−5 and ZnOH^{+}/BAS−HZSM−5, respectively. Also the relative binding structures about TMP and LAS are listed in Fig. S3. It can be known that the existence of LAS enhances the acid strengths of BAS, and the stronger LAS acid strength, the stronger BAS acid strength [65]. So the order of acid strengths is AlOH^{2+}/BAS−HZSM−5 > ZnOH^{+}/BAS−HZSM−5 > BAS−HZSM−5.

For methoxy formation, the relationship between the acid strengths of catalysts and Gibbs free energy barriers of methoxy formation is studied. By comparing Gibbs free energy barriers of methoxy formation in BAS−HZSM−5, AlOH^{2+}/BAS−HZSM−5 and ZnOH^{+}/BAS−HZSM−5, the activity of BAS−HZSM−5 is much lower than the AlOH^{2+}/BAS−HZSM−5 and ZnOH^{+}/BAS−HZSM−5, and the Gibbs free energy barrier differences are 162.6 kJ·mol^{-1} in AlOH^{2+}/BAS−HZSM−5 and 116.9 kJ·mol^{-1} in ZnOH^{+}/BAS−HZSM−5 compared to BAS−HZSM−5. The stronger acid strength is included in AlOH^{2+}/BAS−HZSM−5 and ZnOH^{+}/BAS−HZSM−5 becaues of the synergistic effect of LAS/BAS, and they cause the lower Gibbs free energy barriers for methoxy formation compared to BAS−HZSM−5 [66]. In addition, AlOH^{2+}/BAS−HZSM−5 with the strongest acid strength produces the highest activity for methoxy formation with 68.2 kJ·mol^{-1}, which is better than ZnOH^{+}/BAS−HZSM−5 with 113.9 kJ·mol^{-1} and BAS−HZSM−5 with 230.8 kJ·mol^{-1}. Hence the activity of methoxy formation has consistency with the acid strength of zeolites. And the stronger acid strength helps to enhance the activity of methoxy production [66]. This phenomenon further explains the synergistic effect of LAS/BAS can enhance the acid strengths of catalysts, produce the reaction path which differs from that on the isolated BAS. For methoxy formation, Q_C is effectively reduced, D_{C-O} is shortened, and the activity is improved because of the synergistic effect of LAS/BAS.

Further combined with the above analysis of the acid strengths and the methylation process in three catalysts, it can be found that BAS−HZSM−5 with the weakest acid strength is not beneficial to the formation of methoxy. However, ZnOH^{+}/BAS−HZSM−5 with the moderate acidity is conducive to the formation of methoxy and PX.
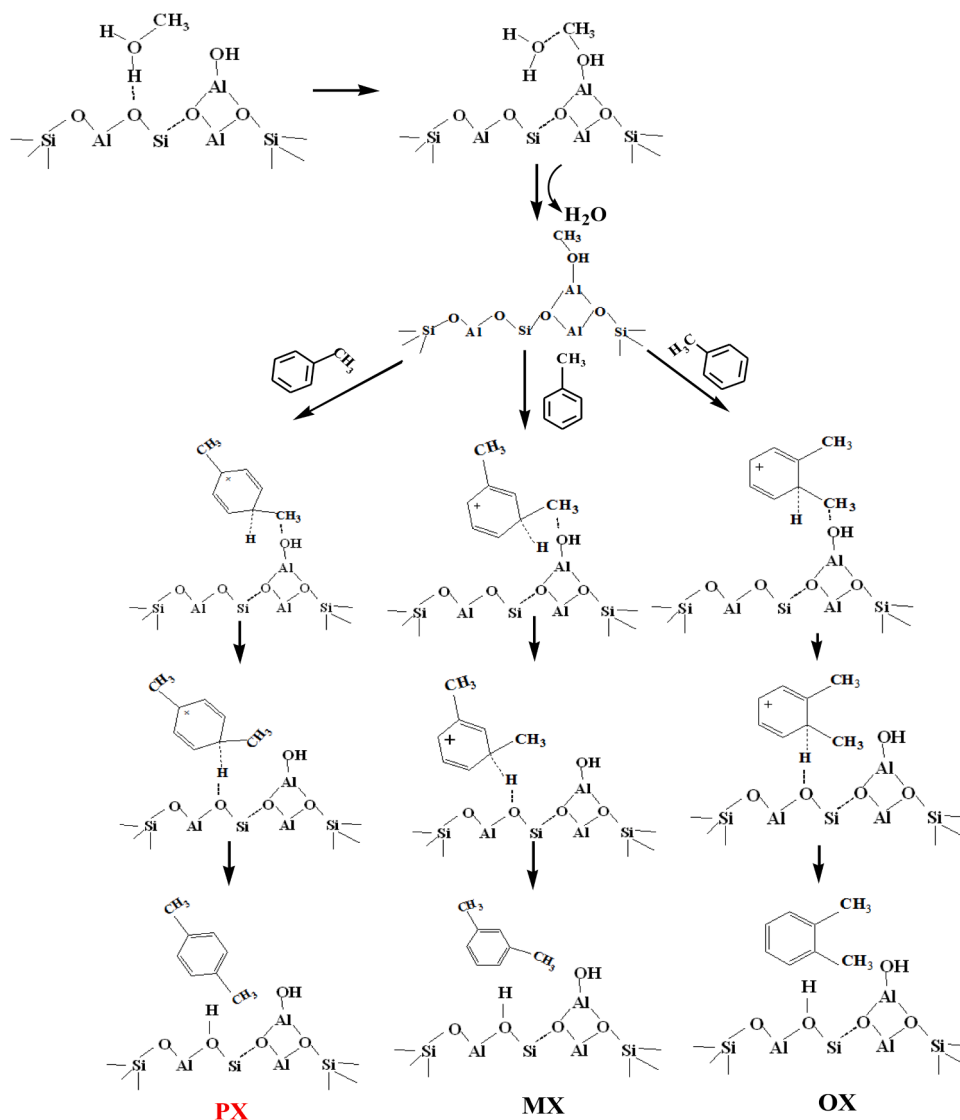
Scheme 2. The reaction route of methylation of toluene with methanol to xylenes in LAS/BAS−HZSM−5.

4. Conclusion

The methylation reaction of methanol and toluene to xylenes are carried out in BAS−HZSM−5, $AlOH^{2+}$/BAS−HZSM−5 and $ZnOH^{+}$/BAS−HZSM−5 catalysts by the DFT method. The reliability of 46T cluster model is verified and which has been selected as the study model. The whole methylation reaction consists of methoxy formation via methanol dissociating and the methylation process of methoxy and toluene to xylenes, and the $C_8H_{11}^{+}$ is the important intermediate for the methylation process. On the one hand, the existence of LAS results in the change of dissociation mechanism for methanol. Methoxy is formed and adsorbed at BAS of BAS−HZSM−5. However, methanol adsorbs at BAS, while the dissociated methoxy transfers from BAS to $AlOH^{2+}$ of $AlOH^{2+}$/BAS−HZSM−5, and $ZnOH^{+}$ of $ZnOH^{+}$/BAS−HZSM−5 with the synergistic effect of LAS/BAS. Moreover, the higher dissociation activity to methanol are exhibited in $AlOH^{2+}$/BAS−HZSM−5 and $ZnOH^{+}$/BAS−HZSM−5 with the higher acid strengths, the less Q_C and the shorter $D_{C−O}$. However, the highest Gibbs free energy barrier for methanol dissociation in BAS−HZSM−5 catalyst is not conductive to the formation of methoxy and PX. On the other hand, the higher Gibbs free energy barrier for PX formation with 129.2 kJ·mol^{-1} needs to be overcome in $AlOH^{2+}$/BAS−HZSM−5 than $ZnOH^{+}$/BAS−HZSM−5 with 92.9 kJ·mol^{-1}. And the formation of PX is easiest among three xylenes in $ZnOH^{+}$/BAS−HZSM−5. It can be seen that $ZnOH^{+}$/BAS−HZSM−5 with the moderate acid strength is conducive to the formation of methoxy and PX. This result will provide a direction to construct an efficient catalyst for the formation of PX in the methylation reaction.

Declaration of Competing Interest

The authors declare that they have no known competing financial interests or personal relationships that could have appeared to influence the work reported in this paper.

CRediT authorship contribution statement

Min Han: Investigation, Data curation, Writing-original draft, Formal analysis, Validation. **Zhongzhong Xue:** Investigation, Data curation, Validation. **Lixia Ling:** Conceptualization, Investigation, Methodology, Formal analysis, Funding acquisition, Writing-review & editing. **Riguang Zhang:** Methodology, Funding acquisition. **Maohong Fan:** Writing-review & editing. **Baojun Wang:** Resources, Funding acquisition, Supervision, Software.

Supplementary materials

Supplementary material associated with this article can be found, in the online version, at doi:10.1016/j.mcat.2021.111622.

References

[1] Z.H. Wen, D.Q. Yang, F. Yang, Z.H. Wei, X.D. Zhu, Methylation of toluene with methanol over HZSM−5: a periodic density functional theory investigation, Chinese J. Catal. 37 (2016) 1882–1890.

[2] D.V. Vu, M. Miyamoto, N. Nishiyama, Y. Egashira, K. Ueyama, Selective formation of para-xylene over H-ZSM-5 coated with polycrystalline silicalite crystals, J. Catal. 243 (2006) 389–394.

[3] J.H. Ahn, R. Kolvenbach, S.S. Al-Khattaf, A. Jentys, J.A. Lercher, Enhancing shape selectivity without loss of activity-novel mesostructured ZSM5 catalysts for methylation of toluene to p-xylene, Chem. Commun. 49 (2013) 10584–10586.

[4] S. Kulprathipanja, Zeolites in industrial separation and catalysis, John Wiley & Sons, 2010.

[5] Y.V. Joshi, K.T. Thomson, Brønsted acid catalyzed cyclization of C7 and C8 dienes in HZSM−5: a hybrid QM/MM study and comparison with C6 diene cyclization, J. Phys. Chem. C 112 (2008) 12825–12833.

[6] J.G. Zhang, W.Z. Qian, C.Y. Kong, F. Wei, Increasing para-xylene selectivity in making aromatics from methanol with a surface-modified Zn/P/ZSM-5 catalyst, ACS Catal. 5 (2015) 2982–2988.

[7] U. Olsbye, S. Svelle, M. Bjorgen, P. Beato, T.V.W. Janssens, F. Joensen, S. Bordiga, K.P. Lillerud, Umwandlung von methanol in kohlenwasserstoffe: wie zeolith-Hohlraume und porengroße die produktselektivitat bestimmen, Angew. Chem. 124 (2012) 2–26.

[8] T. Wang, X.P. Tang, X.F. Huang, W.Z. Qian, Y. Cui, X.Y. Hui, W. Yang, F. Wei, Conversion of methanol to aromatics in fluidized bed reactor, Catal. Today 233 (2014) 8–13.

[9] T.C. Tsai, S.B. Liu, I. Wang, Disproportionation and transalkylation of alkylbenzenes over zeolite catalysts, Appl. Catal. A 181 (1999) 355–398.

[10] J. Shi, Y.D. Wang, W.M. Yang, Y. Tang, Z.K. Xie, Recent advances of pore system construction in zeolite-catalyzed chemical industry processes, Chem. Soc. Rev. 44 (2015) 8877–8903.

[11] J.C. Zuo, W.K. Chen, J. Liu, X.P. Duan, L.M. Ye, Y.Z. Yuan, Selective methylation of toluene using CO₂ and H₂ to para-xylene, Sci. Adv. 6 (2020) 5433–5441.

[12] J. Zhou, Y.D. Wang, W. Zou, C.M. Wang, L.Y. Li, Z.C. Liu, A.M. Zheng, D.J. Kong, W.M. Yang, Z.K. Xie, Mass transfer advantage of hierarchical zeolites promotes methanol converting into para-methyl group in toluene methylation, Ind. Eng. Chem. Res. 56 (2017) 9310–9321.

[13] R.Kolvenbach J.H.Ahn, O.Y. Gutiérrez, S.S. Al-Khattaf, A. Jentys, J.A. Lercher, Tailoring p-xylene selectivity in toluene methylation on medium pore-size zeolites, Micropor. Mesopor. Mat. 210 (2015) 52–59.

[14] Z.R. Zhu, Q.L. Chen, Z.K. Xie, W.M. Yang, C. Li, The roles of acidity and structure of zeolite for catalyzing toluene alkylation with methanol to xylene, Micropor. Mesopor. Mat. 88 (2006) 16–21.

[15] F. Mohammadparast, R. Halladj, S. Askari, The crystal size effect of nano-sized ZSM-5 in the catalytic performance of petrochemical processes: a review, Chem. Eng. Commun. 202 (2015) 542–556.

[16] http://www.iza-structure.org/databases/.

[17] D.C. Li, B. Xing, B.J. Wang, R.F. Li, Activity and selectivity of methanol-to -olefin conversion over Zr-modified H-SAPO-34/H-ZSM-5 zeolites - A theoretical study, Fuel Process. Technol. 199 (2020), 106302.

[18] L.Z. Yang, Z.Y. Liu, Z. Liu, W.Y. Peng, Y.Q. Liu, C.G. Liu, Correlation between H-ZSM-5 crystal size and catalytic performance in the methanol-to-aromatics reaction, Chinese J. Catal. 38 (2017) 683–690.

[19] Y.K. Zhang, Y.X. Qu, D.L. Wang, X.C. Zeng, J.D. Wang, Cadmium modified HZSM−5: a highly efficient catalyst for selective transformation of methanol to aromatics, Ind. Eng. Chem. Res. 56 (2017) 12508–12519.

[20] X.J. Niu, J. Gao, K. Wang, Q. Miao, M. Dong, G.F. Wang, W.B. Fan, Z.F. Qin, J. G. Wang, Influence of crystal size on the catalytic performance of H-ZSM-5 and Zn/H-ZSM-5 in the conversion of methanol to aromatics, Fuel. Process. Tech. 157 (2017) 99–107.

[21] E. El-Malki, R.A. Santen, W.M.H. Sachtler, Introduction of Zn, Ga, and Fe into HZSM−5 cavities by sublimation: identification of acid sites, J. Phys. Chem. B 103 (1999) 4611–4622.

[22] A.S. Al-Dughaither, H.D. Lasa, HZSM-5 zeolites with different SiO₂/Al₂O₃ ratios. characterization and NH₃ desorption kinetics, Ind. Eng. Chem. Res. 53 (2014) 15303–15316.

[23] M. Ravi, V.L. Sushkevich, J.A. Bokhoven, Towards a better understanding of Lewis acidic aluminium in zeolites, Nat. Mater. 19 (2020) 1047–1056.

[24] P. Sazama, B. Wichterlova, J. Dedecek, Z. Tvaruzkova, Z. Musilova, L. Palumbo, S. Sklenak, O. Gonsiorova, FTIR and 27Al MAS NMR analysis of the effect of framework Al- and Si-defects in micro- and micro-mesoporous H-ZSM-5 on conversion of methanol to hydrocarbons, Micropor. Mesopor. Mat. 143 (2011) 87–96.

[25] K. Ramesh, C. Jie, Y.F. Han, A. Borgna, Synthesis, characterization, and catalytic activity of phosphorus modified H-ZSM-5 catalysts in selective ethanol dehydration, Ind. Eng. Chem. Res. 49 (2010) 4080–4090.

[26] G. Kresse, J. Furthmüller, Efficiency of ab-initio total energy calculations for metals and semiconductors using a plane-wave basis set, Comp. Mater. Sci. 6 (1996) 15–50.

[27] D. Wang, C.M. Wang, G. Yang, Y.J. Du, W.M. Yang, First-principles kinetic study on benzene alkylation with ethanol vs. ethylene in H-ZSM-5, J. Catal. 374 (2019) 1–11.

[28] J. Hajek, J.V. Mynsbrugge, K.D. Wispelaere, P. Cnudde, L. Vanduyfhuys, M. Waroquier, V.V. Speybroeck, On the stability and nature of adsorbed pentene in Bronsted acid zeolite H-ZSM-5 at 323, K. J. Catal. 340 (2016) 227–235.

[29] J.P. Perdew, K. Burke, M. Ernzerhof, Generalized gradient approximation made simple, Phys. Rev. Lett. 77 (1996) 3865–3868.

[30] T. Demuth, P. Raybaud, S. Lacombe, H. Toulhoat, Effects of zeolite pore sizes on the mechanism and selectivity of xylene disproportionation-a DFT study, J. Catal. 222 (2004) 323–337.

[31] Y.B. Xu, C.M. Shi, B. Liu, T. Wang, J. Zheng, W.P. Li, D.P. Liu, X.H. Liu, Selective production of aromatics from CO₂, Catal. Sci. Technol. 9 (2019) 593–610.

[32] C.J. Shang, B. Xu, X.L. Lei, S.C. Yu, D.C. Chen, M.S. Wu, B.Z. Sun, G. Liu, C. Y. Ouyang, Bandgap tuning in MoSSe bilayers: synergistic effects of dipole moment and interlayer distance, Phys. Chem. Chem. Phys. 20 (2018) 20919–20926.

[33] L.X. Ling, Y.T. Cao, M. Han, P. Liu, R.G. Zhang, B.J. Wang, Catalytic performance of Pdₙ (n = 1, 2, 3, 4 and 6) clusters supported on TiO₂-ᵥ for the formation of dimethyl oxalate via the CO catalytic coupling reaction: a theoretical study, Phys. Chem. Chem. Phys. 22 (2020) 4549–4560.

[34] X. Rozanska, R. Santen, F. Hutschka, J. Hafner, A periodic DFT study of intramolecular isomerization reactions of toluene and xylenes catalyzed by acidic mordenite, J. Am. Chem. Soc. 123 (2001) 7655–7667.

[35] W.L. Dai, L. Yang, C.M. Wang, X. Wang, G.J. Wu, N.J. Guan, U. Obenaus, M. Hunger, L.D. Li, Effect of n-Butanol cofeeding on the methanol to aromatics conversion over Ga-Modified nano H-ZSM-5 and its mechanistic interpretation, ACS Catal. 8 (2018) 1352–1362.

[36] G.R. Wang, L. Huang, W. Chen, J. Zhang, A.M. Zheng, Rationally designing mixed Cu-(μ-O)-M (M= Cu, Ag, Zn, Au) centers over zeolite materials with high catalytic activity towards methane activation, Phys. Chem. Chem. Phys. 20 (2018) 26522–26531.

[37] A.M. Vos, X. Rozanska, R.A. Schoonheydt, R.A. Santen, F. Hutschka, J. Hafner, A theoretical study of the alkylation reaction of toluene with methanol catalyzed by acidic mordenite, J. Am. Chem. Soc. 123 (2001) 2799–2809.

[38] D.M. McCann, D. Lesthaeghe, P.W. Kletnieks, D.R. Guenther, M.J. Hayman, V. V. Speybroeck, M. Waroquier, J.F. Haw, A complete catalytic cycle for supramolecular methanol-to-olefins conversion by linking theory with experiment, Angew. Chem. 120 (2008) 5257–5260.

[39] V.V. Speybroeck, J.V. Mynsbrugge, M. Vandichel, K. Hemelsoet, D. Lesthaeghe, A. Ghysels, G.B. Marin, M. Waroquier, First principle kinetic studies of zeolite-catalyzed methylation reactions, J. Am. Chem. Soc. 133 (2011) 888–899.

[40] Y.Y. Chu, X.F. Yi, C.B. Li, X.Y. Sun, A.M. Zheng, Brønsted/Lewis acid sites synergistically promote the initial C-C bond formation in the MTO reaction, Chem. Sci. 9 (2018) 6470–6479.

[41] Z.H. Wen, T.F. Xia, M.H. Liu, K.K. Zhu, X.D. Zhu, Methane formation mechanism in methanol to hydrocarbon process: a periodic density functional theory study, Catal. Commun. 75 (2016) 45–49.

[42] N. Hansen, T. Kerber, J. Sauer, A.T. Bell, F.J. Keil, Quantum chemical modeling of benzene ethylation over H-ZSM-5 approaching chemical accuracy: a hybrid MP2: DFT study, J. Am. Chem. Soc. 132 (2010) 11525–11538.

[43] L.A. Clark, M. Sierka, J. Sauer, Computational elucidation of the transition state shape selectivity phenomenon, J. Am. Chem. Soc. 126 (2004) 936–947.

[44] C.J.A. Mota, D.L. Bhering, N. Rosenbach, A DFT study of the acidity of ultrastable Y zeolite: where is the Brønsted/Lewis acid synergism? Angew. Chem. Int. Ed. 43 (2004) 3050–3053.

[45] D.L. Bhering, A. Ramírez-Solís, C.J.A. Mota, A density functional theory based approach to extraframework aluminum species in zeolites, J. Phys.Chem. B 107 (2003) 4342–4347.

[46] A.A. Rybakov, A.V. Larin, G.M. Zhidomirov, Influence of alkali cations on the inter-conversion of extra-framework aluminium species in dealuminated zeolites, Micropor. Mesopor. Mat. 189 (2014) 173–180.

[47] J. Gao, C.L. Wei, M. Dong, G.F. Wang, Z.K. Li, Z.F. Qin, J.G. Wang, W.B. Fan, Evolution of Zn species on Zn/HZSM−5 catalyst under H₂ pretreated and its effect on ethylene aromatization, ChemCatChem 11 (2019) 3892–3902.

[48] P. Zhang, X.J. Yang, X.L. Hou, J.L. Mi, Z.Z. Yuan, J. Huang, C. Stampfl, Active sites and mechanism of the direct conversion of methane and carbon dioxide to acetic acid over the zinc-modified H-ZSM-5 zeolite, Catal. Sci. Technol. 9 (2019) 6297–6307.

[49] A.J. Jones, E. Iglesia, The strength of Brønsted acid sites in microporous aluminosilicates, ACS Catal 5 (2015) 5741–5755.

[50] B.D. Montejo-Valencia, J.L. Salcedo-Pérez, M.C. Curet-Arana, DFT study of closed and open sites of BEA, FAU, MFI, and BEC zeolites substituted with Tin and Titanium, J. Phys. Chem. C 120 (2016) 2176–2186.

[51] S. Wang, Y.Y. Chen, Z.H. Wei, Z.F. Qin, H. Ma, M. Dong, J.F. Li, W.B. Fan, J. G. Wang, Polymethylbenzene or Alkene Cycle? Theoretical Study on Their

Contribution to the Process of Methanol to Olefins over H-ZSM-5 Zeolite, J. Phys. Chem. C 119 (2015) 28482–28498.

[52] Y.V. Joshi, K.T. Thomson, Embedded cluster (QM/MM) investigation of C6 diene cyclization in HZSM−5, J. Catal. 230 (2005) 440–463.

[53] J. Andzelm, N. Govind, G. Fitzgerald, A. Maiti, DFT study of methanol conversion to hydrocarbons in a zeolite catalyst, Int. J. Quantum Chem. 91 (2003) 467–473.

[54] C.M. Zicovich-Wilson, P. Viruela, A. Corma, Formation of surface methoxy groups on H-Zeolites from methanol. A quantum chemical study, J. Phys. Chem. 99 (1995) 13224–13231.

[55] K.Z. Chen, M. Abdolrhamani, E. Sheets, J. Freeman, G. Ward, J.L. White, Direct detection of multiple acidic proton sites in zeolite HZSM-5, J. Am. Chem. Soc. 139 (2017) 18698–18704.

[56] L.L. Yu, S.J. Huang, S. Zhang, Z.N. Liu, W.J. Xin, S.J. Xie, L.Y. Xu, Transformation of isobutyl alcohol to aromatics over zeolite-based catalysts, ACS Catal 2 (2012) 1203–1210.

[57] Bo. Yu, C.M. Ding, J.W. Wang, Y.K. Zhang, Y.Y. Meng, J.X. Dong, H. Ge, X.K. Li, Dual effects of zinc species on active sites in bifunctional composite catalysts Zr/H [Zn] ZSM-5 for alkylation of benzene with syngas, J. Phys. Chem. C 123 (2019) 18993–19004.

[58] S. Müller, Y. Liu, F.M. Kirchberger, M. Tonigold, M. Sanchez-Sanchez, J.A. Lercher, Hydrogen transfer pathways during zeolite catalyzed methanol conversion to hydrocarbons, J. Am. Chem. Soc. 138 (2016) 15994–16003.

[59] F. Schüßler, S. Schallmoser, H. Shi, G.L. Haller, E. Ember, J.A. Lercher, Enhancement of dehydrogenation and hydride transfer by La^{3+} cations in zeolites during acid catalyzed alkane reactions, ACS Catal 4 (2014) 1743–1752.

[60] T. Maihom, B. Boekfa, J. Sirijaraensre, T. Nanok, M. Probst, J. Limtrakul, Reaction mechanisms of the methylation of ethene with methanol and dimethyl ether over H-ZSM-5: an ONIOM study, J. Phys. Chem. C 113 (2009) 6654–6662.

[61] S. Schallmoser, T. Ikuno, M.F. Wagenhofer, R. Kolvenbach, G.L. Haller, M. Sanchez-Sanchez, J.A. Lercher, Impact of the local environment of Brønsted acid sites in ZSM-5 on the catalytic activity in n-pentane cracking, J. Catal. 316 (2014) 93–102.

[62] Y.Y. Chu, N.H. Xue, B.L. Xu, Q. Ding, Z.C. Feng, A.M. Zheng, F. Deng, Mechanism of alkane H/D exchange over zeolite H-ZSM-5 at low temperature: a combined computational and experimental study, Catal. Sci. Technol. 6 (2016) 5350–5363.

[63] Y.Y. Chu, Z.W. Yu, A.M. Zheng, H.J. Fang, H.L. Zhang, S.J. Huang, S.B. Liu, F. Deng, Acidic strengths of Brønsted and Lewis acid sites in solid acids scaled by 31P NMR chemical shifts of adsorbed trimethylphosphine, J. Phys. Chem. C 115 (2011) 7660–7667.

[64] J. Guan, X.J. Li, G. Yang, W.P. Zhang, X.C. Liu, X.W. Han, X.H. Bao, Interactions of phosphorous molecules with the acid sites of H-Beta zeolite: insights from solid-State NMR techniques and theoretical calculations, J. Mol. Catal. A 310 (2009) 113–120.

[65] P. Gao, Q. Wang, J. Xu, G.D. Qi, C. Wang, X. Zhou, X.L. Zhao, N.D. Feng, X.L. Liu, F. Deng, Brønsted/Lewis acid synergy in methanol-to-aromatics conversion on Ga-modified ZSM-5 zeolites, as studied by solid-State NMR spectroscopy, ACS Catal. 8 (2018) 69–74.

[66] L.L. Li, R. Chen, J. Dai, Y. Sun, Z.L. Zhang, X.L. Li, X.W. Nie, C.S. Song, X.W. Guo, Reaction mechanism of benzene methylation with methanol over H-ZSM-5 catalys, Acta Phys. Chim. Sin. 33 (2017) 769–779.